Structure
Article

Structure of Synaptophysin: A Hexameric MARVEL-Domain Channel Protein

Christopher P. Arthur[1] and Michael H.B. Stowell[1,*]
[1] MCD Biology, University of Colorado, Boulder, CO 80309, USA
*Correspondence: stowellm@colorado.edu
DOI 10.1016/j.str.2007.04.011

SUMMARY

Synaptophysin I (SypI) is an archetypal member of the MARVEL-domain family of integral membrane proteins and one of the first synaptic vesicle proteins to be identified and cloned. Most all MARVEL-domain proteins are involved in membrane apposition and vesicle-trafficking events, but their precise role in these processes is unclear. We have purified mammalian SypI and determined its three-dimensional (3D) structure by using electron microscopy and single-particle 3D reconstruction. The hexameric structure resembles an open basket with a large pore and tenuous interactions within the cytosolic domain. The structure suggests a model for Synaptophysin's role in fusion and recycling that is regulated by known interactions with the SNARE machinery. This 3D structure of a MARVEL-domain protein provides a structural foundation for understanding the role of these important proteins in a variety of biological processes.

INTRODUCTION

Neurotransmitter release is a highly regulated process comprised of a series of steps that include the targeting of synaptic vesicles (SVs) to presynaptic active zones, the anchoring of SVs to the plasma membrane, the fusion of the SV membrane with the plasma membrane upon stimulation, and the recycling of the SV membrane and machinery back into a functional SV (Sudhof, 2000). The process of exocytosis during neurotransmitter release has been studied extensively, and several conserved families of proteins have been shown to reside within the SV membrane (De Camilli and Jahn, 1990). One such protein is Synaptophysin I (SypI), which comprises ~8% of all SV proteins (Rehm et al., 1986). SypI is a member of the physin family, which consists of Synaptophysin, Synaptoporin, Pantophysin (SypII), and Mitsugumin (SypIII) (Janz et al., 1999; Leube, 1994) (Figure 1A). While a definitive role of Physins and Synaptogyrins in the vesicle cycle is lacking, evidence indicates that they are components of the vesicle-trafficking machinery (Janz et al., 1999). Physiologically, it has been observed that SypI undergoes a major cellular redistribution in schizophrenia (Eastwood and Harrison, 2001), although how this relates to the disease is unclear.

SypI is a 38 kDa integral membrane protein that is a member of the MARVEL (MAL and related proteins for vesicle trafficking and membrane link) family of integral membrane proteins associated with membrane juxtapositions (Sanchez-Pulido et al., 2002). Based on amino acid sequences, the predicted secondary structure of mammalian SypI consists of four transmembrane α helices, two intravesicular loops, and cytoplasmic N and C termini. The C terminus contains a Ca^{2+}-binding motif and ten pentapeptide repeats, nine of which contain tyrosine residues that are phosphorylated by Src in vitro (Evans and Cousin, 2005; Rehm et al., 1986).

Although SypI is the most abundant protein on SVs, surprisingly little is known about its involvement in the SV cycle or its physiological role in neurotransmitter release. Several experiments have been performed in an attempt to explain SypI's function. Because of Synaptophysin's interaction with the v-SNARE Synaptobrevin (Syb), early studies proposed that it was a negative regulator of vesicle fusion (Becher et al., 1999). Studies in *Xenopus* oocyte-reconstitution systems suggested that SypI has a role in neurotransmitter release, but the precise role was unclear (Valtorta et al., 2004). In contrast, studies of SypI knockout mice showed no pronounced phenotype, and, presumably, SypI had no distinct function in the vesicle cycle (Eshkind and Leube, 1995; Janz et al., 1999). While at least three other isoforms of SypI have been identified that could developmentally compensate for the loss of SypI activity, it appears that, at least transcriptionally, this is not the case (Bai et al., 2006). Intriguingly, a double knockout of SypI and Synaptogyrin shows a pronounced reduction in synaptic plasticity even though evoked neurotransmitter release was still apparently normal. Electron microscopy examination of the morphology of retinal photoreceptors in the SypI/Synaptogyrin knockout mice revealed a defect in SV endocytosis (Spiwoks-Becker et al., 2001; Valtorta et al., 2004), and an increase in the number of clathrin-coated vesicles suggested a selective inhibition of clathrin-independent endocytosis. Further evidence for SypI's involvement in SV endocytosis is that the major SypI-binding partner on SVs, Syb, has been implicated in a form of endocytosis that rapidly recycles SVs after exocytosis (Dittman and Kaplan, 2006). Regardless of the precise function of SypI, it must participate in the vesicle cycle at some stage,

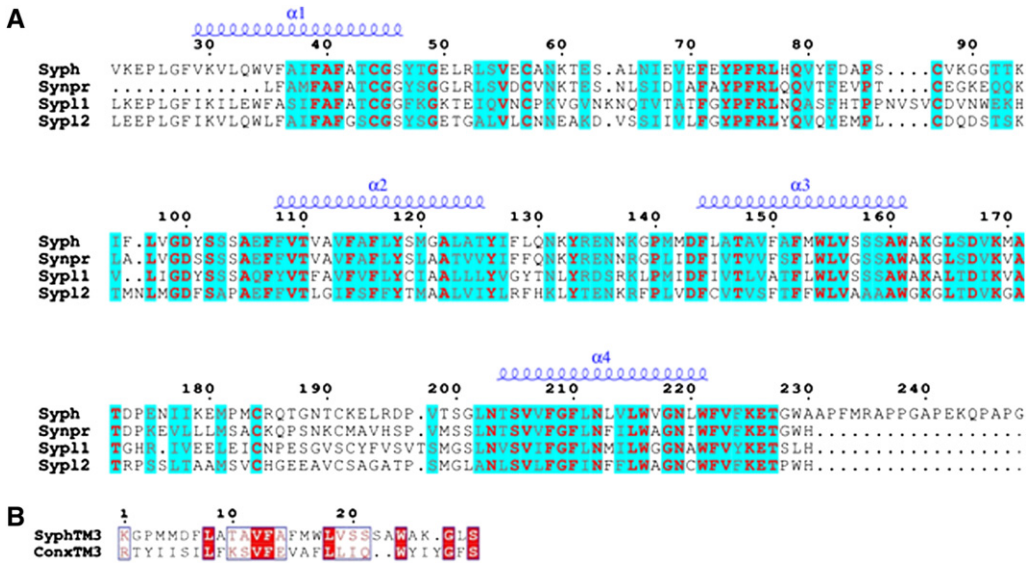

Figure 1. Comparison of Transmembrane Domains of Synaptophysin-Family Proteins and Sequence Alignment of Synaptophysin and Connexin

(A) Sequences are taken from mouse Synaptophysin I (Syph), mouse Synaptoporin (Synpr), mouse Synaptophysin-like protein I (SypII), and mouse Synaptophysin-like protein II (SypIII). These proteins are known to reside on synaptic vesicles and may account for the lack of phenotype seen when individual members of this family are removed.

(B) Sequence alignment of the third transmembrane segment of SypI (SyphTM3) and the third transmembrane segment of Connexin α1 (ConxTM3).

and its identification as a member of the MARVEL family of membrane proteins involved in membrane juxtapositions further suggests that it may have a role in fusion and recycling. While, physiologically, SypI does not have an essential role, it is most likely important for fine tuning of neurotransmitter release, which effects memory and learning phenomenon such as LTP. This higher-order function appears to be related to the phosphorylation of Synaptophysin, which occurs after LTP-stimulation protocols (Evans and Cousin, 2005).

Structurally, SypI has been observed to form a multimer, which, when reconstituted into a planar lipid bilayer, forms voltage-dependent channels with a conductance similar to gap junctions and a mechanosensitive channel (Bass et al., 2002; Gincel and Shoshan-Barmatz, 2002; Perozo et al., 2002; Rehm et al., 1986; Unger et al., 1999). While SypI and the gap junction protein Connexin share very little sequence homology, they do share similar membrane topologies and strong similarity within their third transmembrane domain (Leube, 1995) (Figure 1B). Interestingly, this third transmembrane domain of Connexin lines the gap junction pore and, by analogy, perhaps the fusion pore of SypI. While it has been proposed that SypI may be the main component of a potential fusion pore complex that forms during transient fusion events involving SVs, no structural work has been done to verify that SypI forms a channel-like structure that would be compatible with such a hypothesis (Pennuto et al., 2002; Valtorta et al., 2004). Here, we report the first, to our knowledge, 3D structural analysis of the SypI complex at 20 Å resolution by using negative-stain electron microscopy and computational image processing. The structure reveals that SypI forms a hexameric basket-like complex with a closed conformation on the cytosolic side of the membrane and an extended, open conformation on the vesicle lumen side as well as a large pore within the membrane, and it suggests how SypI may be involved in the vesicle cycle.

RESULTS

The SypI structure resembles multimeric mechanosensitive channels and gap junction hemichannels and is consistent with the hypothetical role of SypI as a neurotransmitter channel that disassociates during vesicle fusion. The 3D map generated for SypI (Figure 2C) has dimensions of ~70 Å × ~70 Å (overall height × diameter) and an enclosed volume of ~226,000 Å^3. This is comparable to the calculated volume for a 240 kDa SypI hexamer (~197,000 Å^3) (Fischer et al., 2004). The structure shows a basket-like formation with six individual spokes of density radiating outward and upward from a central hub. The structure also shows an apparent handedness that is seen in many biological structures (Bass et al., 2002; Perozo et al., 2002). During the reconstruction, a six-fold symmetry was imposed to generate the final 3D map. Results of crosslinking analysis along with gel-filtration chromatography of the purified SypI complex led us to believe that SypI indeed exists as a hexamer in vivo (Figure 3A). In order to verify that our final reconstruction was accurate, we performed subsequent reconstructions with the same data, but by imposing either five-fold or seven-fold symmetry (Figure 3D). Neither of these reconstructions generated a coherent model.

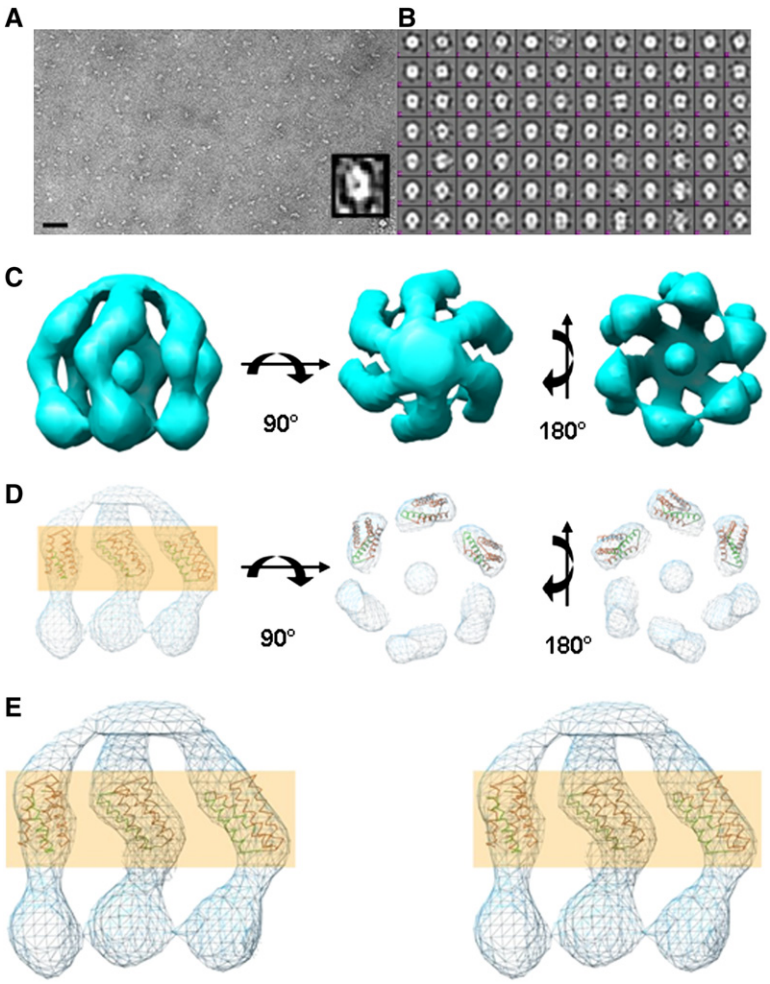

Figure 2. Single-Particle Electron Microscopy of Negatively Stained Synaptophysin I

(A) Low-dose image of Synaptophysin I complexes negatively stained with 2% ammonium molybdate on continuous carbon substrate. (Inset) Magnified image of a single Synaptophysin I complex (the scale bar is 100 nm).

(B) Gallery of representative class averages displaying various views of the Synaptophysin I complex.

(C) Three views of the surface-rendered density map of the Synaptophysin I complex rendered at 20 Å resolution. The structure shows an overall diameter of 70 Å and an inner diameter of 30 Å. Density is contoured to 2.0σ.

(D) Mesh view of (C) with Connexin docked into the density map. The highlighted area represents the lipid bilayer.

(E) Stereo mesh view of (D) truncated to show the inner wall of the complex. The atomic model of Connexin is docked into the density map; the third transmembrane domain is represented in green. The highlighted area represents the lipid bilayer.

Based on the predicted membrane topology of SypI (Figure 1A) and its similarity to the gap junction complex, we were able to dock a previously determined model (Fleishman et al., 2004) of the transmembrane segment of the gap junction into our density map (Figures 2D and 2E). The docking allows us to delineate the area of the plasma membrane and assign an orientation of SypI. Based on the amino acid sequence and expected volume occupied by the intratransmembrane loops, we have assigned the open end of the structure within the vesicle lumen, and the closed end containing the N and C termini on the cytosolic side of the vesicle membrane (Figures 2C–2E). The third transmembrane domain of Connexin has been shown to line the gap junction pore, and, by analogy, we docked the transmembrane domain structure in a similar orientation, allowing for the possibility that the third transmembrane domain of SypI may line the interior of the SypI fusion pore complex.

DISCUSSION

The intermediate resolution model that we have generated bares a striking resemblance to other known channel structures, in particular the gap junction and mechanosensitive channels, both of which have similar conductances as the SypI channel (Figure 4). The overall dimensions of these channels are quite similar as well. Our SypI structure has an outer diameter of ~70 Å and an inner diameter of ~30 Å; these dimensions are similar to those of Connexin (Unger et al., 1999) and are very similar to the dimensions of MscS (80 Å diameter, 25 Å pore) (Bass et al., 2002). The apparently loose intersubunit/intramembrane interactions suggest how SypI may interact with Syb and function as a mechanosensitive channel in which SNARE-complex formation drives disassembly of the SypI/Syb multimer, leading to channel opening and neurotransmitter release (Figure 5). Recent work has shown that the fusion pore involved in neurotransmitter release has a conductance of > 375 pS, and that the potential pore diameter based on this conductance should be in the order of > 2.3 nm (He et al., 2006). These numbers correlate very well with the 3D structure that we have generated.

There are two observed mechanisms of vesicle fusion and recycling at the presynaptic active zone: full fusion and transient fusion (also known as kiss-and-run) (Sudhof, 2000). In the full-fusion model, SVs are docked at the presynaptic membrane by a potential interaction of Syb

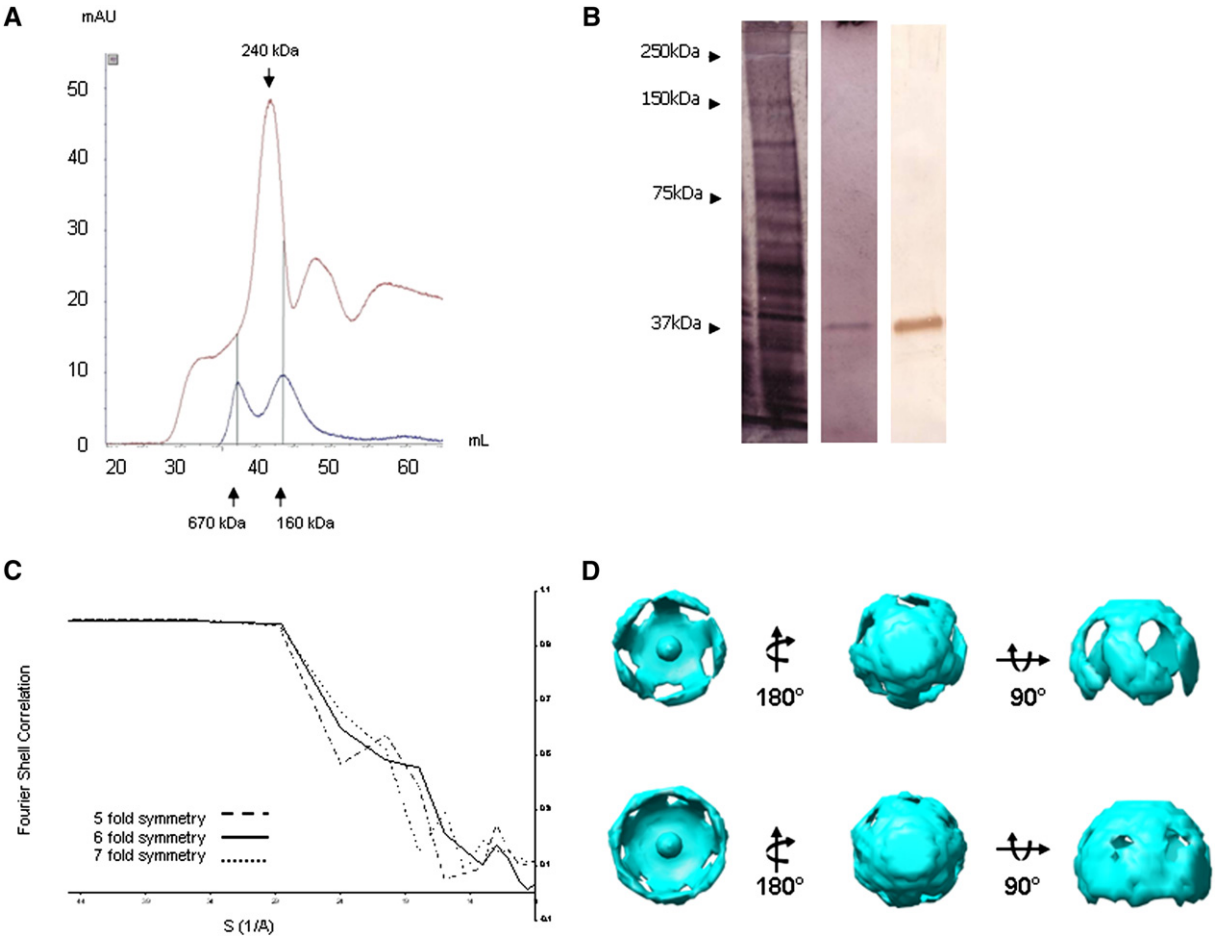

Figure 3. Chromatogram from Gel-Filtration Purification of the Synaptophysin I Complex

Resolution analysis of the Synaptophysin I 3D reconstruction and models of five-fold and seven-fold imposed symmetry. Resolution analysis of Synaptophysin I 3D reconstruction and models of five-fold and seven-fold imposed symmetry.

(A) Chromatogram from gel-filtration purification of the Synaptophysin I complex. The blue curve shows calibration standards for the purification column run under Synaptophysin I-isolation conditions. Arrows point to peaks representing 670 kDa and 160 kDa. The red curve shows gel filtration of solubilized Synaptophysin I complex isolated from bovine brain tissue. The arrow points to the peak representing the 240 kDa Synaptophysin I complex, as verified by SDS-PAGE and western blot analysis.

(B) SDS-PAGE analysis of (L-R) purified synaptic vesicles, the final purified Synaptophysin I complex, and western blot analysis of the purified complex. Arrows show marked molecular weights.

(C) Fourier shell correlation curve showing the calculated resolution of the reconstruction to be ~20 Å based on the FSC = 0.5 criterion.

(D) Reconstruction of the same single-particle data shown in Figure 2 with five-fold symmetry imposed. Density is contoured to 0.5σ.

on the vesicle surface and Syntaxin (Syx) on the plasma membrane (Figure 5, step 1). These proteins are thought to potentially be held together by SNAP25 and complexin (Tang et al., 2006). Upon depolarization of the neuronal membrane and influx of Ca^{2+}, Synaptotagmin I (SytI) binds to the SNARE complex, and its Ca^{2+}-binding C2 domains form a tight electrostatic interaction with the plasma membrane. A subsequent coiled coil is formed by the SNARE complex (Syx, Syb, and SNAP25), thus drawing in the SV to fully fuse with the plasma membrane (Figure 5, steps 2 and 3) (Hui et al., 2006). During transient fusion, the SV is also drawn in close to the plasma membrane upon depolarization and Ca^{2+} influx. However, the SV never fully fuses with the plasma membrane; rather, only a transient fusion pore is formed for neurotransmitter release, and the intact SV is eventually released from the membrane and reprimed for another fusion event (Figure 5, steps 2* and 3*). Currently, the molecular mechanism of transient fusion is not known. Multiple proteins, including SypI, have been proposed as contributors and/or regulators of transient fusion; however, the roles of these proteins have not been confirmed (Fernandez-Alfonso and Ryan, 2004; Harata et al., 2006; Wang et al., 2003, 2006).

Based on our structure and published biochemical data on SypI and other SV proteins, including SytI, Syb, Syx, and Synaptotagmin IV (SytIV), we have derived the following model for a possible role of SypI in pore formation during full and transient SV fusion. Syb is known to

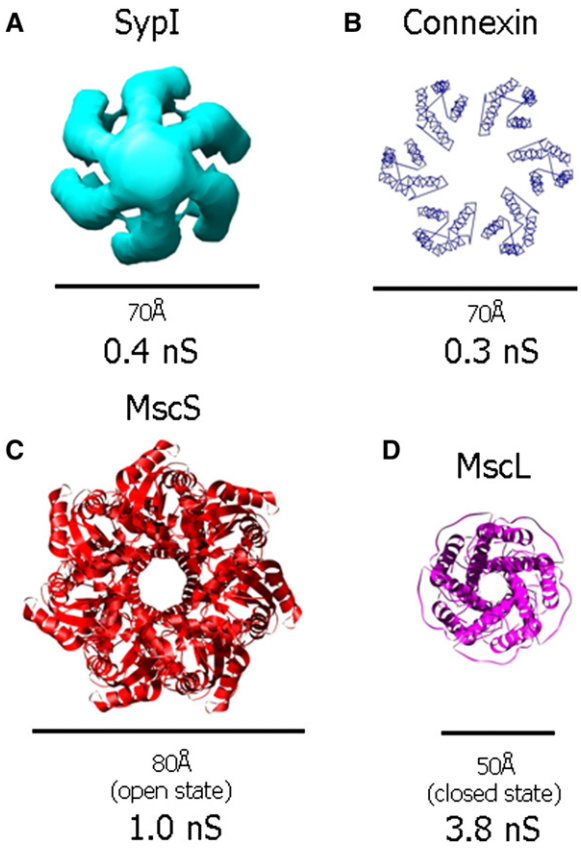

Figure 4. Comparison of the Synaptophysin I Complex with Other Known Channel Structures

(A) The Synaptophysin I complex shows a similar structure and conductance to both Connexin and mechanosensitive channels. Synaptophysin I has an outer diameter of 70 Å and a conductance of 0.4 nS.

(B) Connexin (PDB code: 1TXH) has an outer diameter of 70 Å and a conductance of 0.3 nS.

(C) The small mechanosensitive channel, MscS (PDB code: 2OAU), has an outer diameter of 80 Å and a conductance of 1.0 nS.

(D) The large mechanosensitive channel, MscL (PDB code: 2OAR), has an outer diameter of 50 Å and a conductance of 3.8 nS.

bind to multiple SV proteins, including SypI and SytIV, exclusive of SNARE-complex formation (Fukuda, 2002; Pennuto et al., 2002). SytIV has been implicated in transient fusion (Wang et al., 2003), although to what extent is unclear. Increased expression of SytIV leads to an increase in kiss-and-run events, and removal of SytIV leads to a disability in memory function associated with neurotransmitter release (Ferguson et al., 2000) and a loss of SVs (C. Dean, C.P.A., A. Bhalla, H. Liu, P. Chang, M.H.B.S., M.B. Jackson, and E.R. Chapman, unpublished data). SytIV has also been shown to compete with SytI for SNARE binding (Machado et al., 2004). We propose that the interaction of SytIV with the SypI/Syb complex can regulate the choice between kiss-and-run and full fusion. In our model, Syb and SypI are bound in a multimeric complex with SytIV prior to the SV being docked at the active zone (Figure 5, step 1). Upon membrane depolarization, SytIV binds weakly with the presynaptic membrane; Syb is inhibited by SypI from entering the coiled-coil SNARE complex; and the SypI/Syb complex remains stable, potentially forming a fusion pore with Syx, another complex on the plasma membrane that has been shown to be active in neurotransmitter release (Figure 5, step 2*) (Han et al., 2004). The SytIV/plasma membrane interaction is not as strong as the SytI/plasma membrane interaction, and no full SNARE complex is formed. The Syx/SypI fusion pore dissociates, potentially upon interaction with Dynamin, and the SV does not go through full fusion (Figure 5, step 3*). In this model, the exclusion of SytI from the binding machinery inhibits the vesicle from undergoing complete exocytosis. In the full-fusion model, the strong interaction of SytI with the plasma membrane allows for the formation of the complete SNARE complex, and this strong interaction acts to dissociate Syb from the SypI complex, thus allowing the SypI complex to destabilize and full vesicle fusion to occur (Figure 5, step 3).

The four transmembrane-helix architecture of SypI is observed in a number of proteins, including Myelin and Lymphocyte Protein (MAL), Synaptogyrin, and Occludin (Sanchez-Pulido et al., 2002). The involvement of all of these MARVEL-domain proteins in the processes of membrane contact and interaction is strong evidence for SypI's role in vesicle membrane interaction at the plasma membrane. The structure of SypI described here provides the first, to our knowledge, 3D data for a MARVEL-domain protein and suggests how SypI may form a fusion pore complex that regulates SV exocytosis. While further studies are required to fully elucidate the function and mechanism of SypI, as well as other MARVEL-domain proteins, our results provide a structural foundation for understanding these important and ubiquitous proteins.

EXPERIMENTAL PROCEDURES

SV Preparation

SVs were prepared from frozen calf brain as described previously (Huttner et al., 1983). Briefly, 20 g frozen tissue was homogenized in a buffer solution (4 mM HEPES [pH 7.3], 0.32 M sucrose). Homogenate was centrifuged at 800 × g for 15 min (4°C). Supernatant was removed and centrifuged at 9,200 × g for 20 min (4°C). The pellet was resuspended in an equal volume of homogenization buffer and centrifuged at 10,200 × g for 20 min (4°C). The pellet was resuspended in 40 ml homogenization buffer. The resuspended pellet was diluted 1:10 with ice-cold dH_2O. This suspension was subjected to three up-and-down strokes in a glass homogenizer. The resulting lysate was poured rapidly into 9 ml 1 M HEPES (pH 7.3), and the suspension was incubated on ice for 30 min. The suspension was then centrifuged at 25,000 × g for 20 min (4°C), and the supernatant was removed and centrifuged at 165,000 × g for 2 hr (4°C). The pellet was resuspended in 10 ml 40 mM sucrose, and the suspension was layered on top of a continuous sucrose gradient. The sucrose gradient was centrifuged at 65,000 × g for 5 hr (4°C). At the end of centrifugation, the gradient revealed a broad band of high turbidity at the 200–400 mM sucrose region, which, from previous experiments (Fukuda, 2002), is known to be enriched in SVs. This band was collected and further processed for SypI purification.

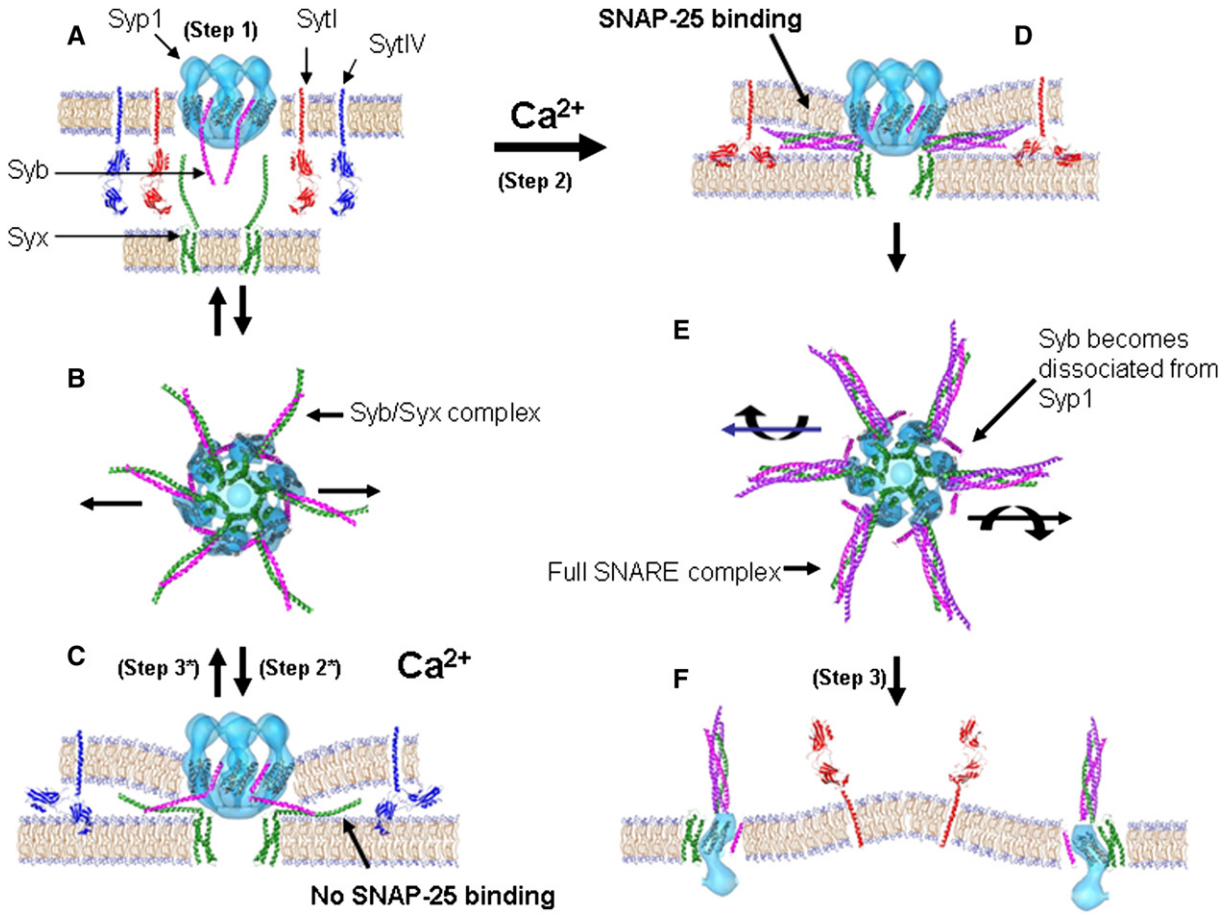

Figure 5. Model for Synaptophysin I Complex Involvement in Vesicle Fusion

(A–F) Vesicles containing unassembled SNARE complexes approach the active zone of the presynaptic matrix. (A) Vesicles become "docked" via the t/v-SNARE interaction (step 1). Vesicles then proceed down one of two pathways: full fusion (FF) or kiss-and-run (KNR). Along the FF pathway SytI is the principal calcium sensor. (E and F) Upon calcium influx, SytI binds to the SNARE complex, and both C2 domains of SytI bind calcium and form a tight electrostatic interaction with the presynaptic membrane, which pulls the vesicle into the presynaptic membrane. The SypI complex then binds with Syx on the plasma membrane and forms a fusion pore (step 2). The strong interaction of SytI with the presynaptic membrane and the tight formation of the SNARE complex disassociates Syb from SypI, thus weakening the SypI complex and allowing the vesicle to fully fuse and dissociate the SypI hexamer (step 3). (E) Top view of the interaction of the SNARE complex and the dislodging of Syb from the SypI complex. (B and C) In the KNR pathway, SytIV is the principal calcium sensor, and a weak interaction between SytIV and Syb occurs, excluding SytI from interacting with Syb. Upon calcium influx, only the C2B domain of SytIV binds calcium. This results in a weaker electrostatic interaction between SytIV and the presynaptic membrane (step 2*). The weak interaction of SytIV with the presynaptic membrane and the exclusion of Syb from forming a complete SNARE complex allows Syb to remain bound to the SypI complex and inhibits the vesicle from fully fusing (step 3*). (B) Top view of the interaction of Syb with Syx and shows how Syb remains bound to the SypI complex during transient fusion.

SypI Purification

Purified SVs were incubated for 30 min at 0°C (at 5 mg/ml) in a solution containing 5 mM NaH_2PO_4 (pH 6.8) and 0.2% Triton X-100 (w/v). The Triton X-100 extract was centrifuged at 45,000 × g for 30 min (4°C). The supernatant was applied to a dry hydroxyapatite/celite column (2:1 w/w) (0.1 g/mg protein) and eluted with solubilization buffer. The resin-bound proteins were eluted and found to contain no SypI. The SypI containing flowthrough was applied to a POROS H10 anion-exchange column and eluted by using a NaCl gradient from 0 to 1 M (20 mM NaH_2PO_4 [pH 6.8], 0.2% Brij-35, 40 mM sucrose). Fractions (1 ml) were collected and analyzed with SDS-PAGE. Fractions containing SypI were combined and flowed over a Hi-Prep Sephacryl S-300 size-exclusion column. The protein was eluted by using 20 mM NaH_2PO_4 (pH 6.8), 0.2% Brij-35, 40 mM sucrose. Fractions were analyzed with SDS-PAGE and western blot techniques. Blots were probed with monoclonal SypI antibodies. Fractions of purified SypI were combined (Figure 3B).

Electron Microscopy

Purified SypI (50 μg/ml) was applied to a freshly carbon-coated, glow-discharged EM grid and stained with 2% ammonium molybdate (Hoenger and Aebi, 1996). Images were recorded under low-dose conditions at a magnification of 50,000 and at a defocus range of 1–3 μm with a Tecnai F20 microscope at 200 keV equipped with a Gatan 2K × 2K CCD camera. The pixel size was 0.45 nm.

Image Processing

Individual SypI particles were selected and boxed, and image analysis was performed by using the EMAN image processing package (Ludtke et al., 1999). Briefly, an initial model was generated by using the raw

boxed particles and an imposed six-fold symmetry (based on size-exclusion chromatography data that tells us that SypI is a hexamer, Figure 3A). From this initial model, angular projections were generated and particles were again classified based on these projections. From these classifications, a new model was generated and the process was repeated. The final model was a result of 8 rounds of refinement and contained ~1,200 particles. The resolution of the final model was calculated to be ~20 Å based on FSC with a standard cutoff of 0.5 (Figure 3C).

ACKNOWLEDGMENTS

We thank our colleagues at the University of Colorado for their support. We thank E.R. Chapman, A. Hoenger, R.A. Milligan, A.B. Ward, and M.W. Klymkowsky for comments on the manuscript. C.P.A. was supported by the National Institutes of Health (NIH)/University of Colorado Molecular Biophysics Training Program (NIH T32 GM065103). This work was supported in part by the Human Frontier Science Program (M.H.B.S.) and the Beckman Foundation (M.H.B.S.). The EM facilities were supported by a generous gift of the Argouron Institute. The authors declare no competing financial interests.

Received: February 27, 2007
Revised: March 30, 2007
Accepted: April 6, 2007
Published: June 12, 2007

REFERENCES

Bai, L., Spiwoks-Becker, I., and Leube, R.E. (2006). Transcriptome comparison of murine wild-type and synaptophysin-deficient retina reveals complete identity. Brain Res. *1081*, 53–58.

Bass, R.B., Strop, P., Barclay, M., and Rees, D.C. (2002). Crystal structure of *Escherichia coli* MscS, a voltage-modulated and mechanosensitive channel. Science *298*, 1582–1587.

Becher, A., Drenckhahn, A., Pahner, I., Margittai, M., Jahn, R., and Ahnert-Hilger, G. (1999). The synaptophysin-synaptobrevin complex: a hallmark of synaptic vesicle maturation. J. Neurosci. *19*, 1922–1931.

De Camilli, P., and Jahn, R. (1990). Pathways to regulated exocytosis in neurons. Annu. Rev. Physiol. *52*, 625–645.

Dittman, J.S., and Kaplan, J.M. (2006). Factors regulating the abundance and localization of synaptobrevin in the plasma membrane. Proc. Natl. Acad. Sci. USA *103*, 11399–11404.

Eastwood, S.L., and Harrison, P.J. (2001). Synaptic pathology in the anterior cingulate cortex in schizophrenia and mood disorders. A review and a Western blot study of synaptophysin, GAP-43 and the complexins. Brain Res. Bull. *55*, 569–578.

Eshkind, L.G., and Leube, R.E. (1995). Mice lacking synaptophysin reproduce and form typical synaptic vesicles. Cell Tissue Res. *282*, 423–433.

Evans, G.J., and Cousin, M.A. (2005). Tyrosine phosphorylation of synaptophysin in synaptic vesicle recycling. Biochem. Soc. Trans. *33*, 1350–1353.

Ferguson, G.D., Anagnostaras, S.G., Silva, A.J., and Herschman, H.R. (2000). Deficits in memory and motor performance in synaptotagmin IV mutant mice. Proc. Natl. Acad. Sci. USA *97*, 5598–5603.

Fernandez-Alfonso, T., and Ryan, T.A. (2004). The kinetics of synaptic vesicle pool depletion at CNS synaptic terminals. Neuron *41*, 943–953.

Fischer, H., Polikarpov, I., and Craievich, A.F. (2004). Average protein density is a molecular-weight-dependent function. Protein Sci. *13*, 2825–2828.

Fleishman, S.J., Unger, V.M., Yeager, M., and Ben-Tal, N. (2004). A Cα model for the transmembrane α helices of gap junction intercellular channels. Mol. Cell *15*, 879–888.

Fukuda, M. (2002). Vesicle-associated membrane protein-2/synaptobrevin binding to synaptotagmin I promotes O-glycosylation of synaptotagmin I. J. Biol. Chem. *277*, 30351–30358.

Gincel, D., and Shoshan-Barmatz, V. (2002). The synaptic vesicle protein synaptophysin: purification and characterization of its channel activity. Biophys. J. *83*, 3223–3229.

Han, X., Wang, C.T., Bai, J., Chapman, E.R., and Jackson, M.B. (2004). Transmembrane segments of syntaxin line the fusion pore of Ca2+-triggered exocytosis. Science *304*, 289–292.

Harata, N.C., Aravanis, A.M., and Tsien, R.W. (2006). Kiss-and-run and full-collapse fusion as modes of exo-endocytosis in neurosecretion. J. Neurochem. *97*, 1546–1570.

He, L., Wu, X.S., Mohan, R., and Wu, L.G. (2006). Two modes of fusion pore opening revealed by cell-attached recordings at a synapse. Nature *444*, 102–105.

Hoenger, A., and Aebi, U. (1996). 3-D reconstructions from ice-embedded and negatively stained biomacromolecular assemblies: a critical comparison. J. Struct. Biol. *117*, 99–116.

Hui, E., Bai, J., and Chapman, E.R. (2006). Ca2+-triggered simultaneous membrane penetration of the tandem C2-domains of synaptotagmin I. Biophys. J. *91*, 1767–1777.

Huttner, W.B., Schiebler, W., Greengard, P., and De Camilli, P. (1983). Synapsin I (protein I), a nerve terminal-specific phosphoprotein. III. Its association with synaptic vesicles studied in a highly purified synaptic vesicle preparation. J. Cell Biol. *96*, 1374–1388.

Janz, R., Sudhof, T.C., Hammer, R.E., Unni, V., Siegelbaum, S.A., and Bolshakov, V.Y. (1999). Essential roles in synaptic plasticity for synaptogyrin I and synaptophysin I. Neuron *24*, 687–700.

Leube, R.E. (1994). Expression of the synaptophysin gene family is not restricted to neuronal and neuroendocrine differentiation in rat and human. Differentiation *56*, 163–171.

Leube, R.E. (1995). The topogenic fate of the polytopic transmembrane proteins, synaptophysin and connexin, is determined by their membrane-spanning domains. J. Cell Sci. *108*, 883–894.

Ludtke, S.J., Baldwin, P.R., and Chiu, W. (1999). EMAN: semiautomated software for high-resolution single-particle reconstructions. J. Struct. Biol. *128*, 82–97.

Machado, H.B., Liu, W., Vician, L.J., and Herschman, H.R. (2004). Synaptotagmin IV overexpression inhibits depolarization-induced exocytosis in PC12 cells. J. Neurosci. Res. *76*, 334–341.

Pennuto, M., Dunlap, D., Contestabile, A., Benfenati, F., and Valtorta, F. (2002). Fluorescence resonance energy transfer detection of synaptophysin I and vesicle-associated membrane protein 2 interactions during exocytosis from single live synapses. Mol. Biol. Cell *13*, 2706–2717.

Perozo, E., Cortes, D.M., Sompornpisut, P., Kloda, A., and Martinac, B. (2002). Open channel structure of MscL and the gating mechanism of mechanosensitive channels. Nature *418*, 942–948.

Rehm, H., Wiedenmann, B., and Betz, H. (1986). Molecular characterization of synaptophysin, a major calcium-binding protein of the synaptic vesicle membrane. EMBO J. *5*, 535–541.

Sanchez-Pulido, L., Martin-Belmonte, F., Valencia, A., and Alonso, M.A. (2002). MARVEL: a conserved domain involved in membrane apposition events. Trends Biochem. Sci. *27*, 599–601.

Spiwoks-Becker, I., Vollrath, L., Seeliger, M.W., Jaissle, G., Eshkind, L.G., and Leube, R.E. (2001). Synaptic vesicle alterations in rod photoreceptors of synaptophysin-deficient mice. Neuroscience *107*, 127–142.

Sudhof, T.C. (2000). The synaptic vesicle cycle revisited. Neuron *28*, 317–320.

Tang, J., Maximov, A., Shin, O.H., Dai, H., Rizo, J., and Sudhof, T.C. (2006). A complexin/synaptotagmin 1 switch controls fast synaptic vesicle exocytosis. Cell *126*, 1175–1187.

Unger, V.M., Kumar, N.M., Gilula, N.B., and Yeager, M. (1999). Three-dimensional structure of a recombinant gap junction membrane channel. Science *283*, 1176–1180.

Valtorta, F., Pennuto, M., Bonanomi, D., and Benfenati, F. (2004). Synaptophysin: leading actor or walk-on role in synaptic vesicle exocytosis? Bioessays *26*, 445–453.

Wang, C.T., Lu, J.C., Bai, J., Chang, P.Y., Martin, T.F., Chapman, E.R., and Jackson, M.B. (2003). Different domains of synaptotagmin control the choice between kiss-and-run and full fusion. Nature *424*, 943–947.

Wang, C.T., Bai, J., Chang, P.Y., Chapman, E.R., and Jackson, M.B. (2006). Synaptotagmin-Ca^{2+} triggers two sequential steps in regulated exocytosis in rat PC12 cells: fusion pore opening and fusion pore dilation. J. Physiol. *570*, 295–307.

